Cellulose (2020) 27:4787–4802
https://doi.org/10.1007/s10570-020-03074-0

ORIGINAL RESEARCH

The efficient removal of anionic and cationic dyes from aqueous media using hydroxyethyl starch-based hydrogels

Pinar Ilgin · Hava Ozay · Ozgur Ozay

Received: 29 July 2019 / Accepted: 19 February 2020 / Published online: 27 February 2020

Abstract In this study, hydroxyethyl starch (HES)-based hydrogels, hydroxyethyl starch/p(sodium acrylate) (HES/p(NaAAc)), hydroxyethyl starch/p(3-(acrylamidopropyl) trimethyl ammonium chloride) (HES/p(APTMACl)) and hydroxyethyl starch/p(acrylamide) (HES/p(AAm)) were synthesized with redox polymerization. The structural, morphological, and water absorption characterization of the synthesized hydrogels was investigated. HES-based hydrogels, containing anionic, cationic and neutral functional groups, were used for adsorption of methyl violet (MV) as a model cationic dye and methyl orange (MO) as a model anionic dye from aqueous media. HES/p(APTMACl) and HES/p(NaAAc) hydrogels had maximum adsorption values for MO and MV dyes of 238.1 mg/g and 185.2 mg/g. The isotherm and kinetic parameters for both dye adsorptions were determined. The adsorption isotherm and kinetic data were compatible with the Langmuir isotherm and pseudo-first-order kinetic models.

Keywords Dye · Adsorption · Methyl violet · Methyl orange · Hydrogel

P. Ilgin (✉)
Department of Chemistry and Chemical Processing Technologies, Lapseki Vocational School, Canakkale Onsekiz Mart University, Lapseki, Canakkale, Turkey
e-mail: pinarilgin@comu.edu.tr; pinarilgin2014@gmail.com

H. Ozay · O. Ozay
Laboratory of Inorganic Materials, Department of Chemistry, Faculty of Science and Arts, Canakkale Onsekiz Mart University, Canakkale, Turkey

O. Ozay
Department of Bioengineering, Faculty of Engineering, Canakkale Onsekiz Mart University, Canakkale, Turkey

Introduction

In the last one hundred years, rapid urbanization in addition to intensification of industrial activities have been important factors increasing environmental pollution (Mohammed et al. 2015; Bello et al. 2018). The largest factors creating this pollution are organic and inorganic chemicals. In particular, a large number of dyestuffs that pose a danger to the environment are widely used; for example, in the textile, leather and paint industries (Sami et al. 2018; Jana et al. 2018a; Ngwabebhoh et al. 2016). Sometimes these dyes are released as wastewater into the environment without any precautions, resulting in toxic and carcinogenic pollution of the entire ecosystem (Mohamed et al. 2018; Capanema et al. 2018; Hu et al. 2018a; Sami et al. 2017), even at low concentrations. For water resources polluted intensely by organic dyes, phenolic compounds, pesticides and heavy metal ions, many treatment methods are used like microbiological decomposition, photo catalysis, ozonation, membrane

separation, chemical precipitation, oxidation, flocculation, and adsorption (Krishnappa and Badalamoole 2019; Wang et al. 2019; Liang et al. 2019). Among these methods, adsorption is one of the most commonly chosen in recent years due to simple design, high efficiency, low cost and most importantly, the ability to be used repeatedly. (Bhattacharyya and Ray 2014; Zhu et al. 2019).

In the literature, active carbon, resins, a variety of nanomaterials, biosorbents and hydrogels are examples of materials most often used as adsorbents (Hu et al. 2018b; Jv et al. 2019; Pavithra et al. 2019). In addition to all other characteristics of adsorbent materials, the ability to easily remove them from the adsorption medium is very important in terms of cost. This feature brings hydrogels to the forefront, ahead of all other adsorbents (Ilgin et al. 2019a; Ozay et al. 2010). Hydrogel structures are generally known to be modifiable hydrophilic polymers (Ozay et al. 2016; Ozay and Ozay 2013). Hydrogels, with physical or chemical cross-linking, can provide water absorption up to hundreds of times their mass due to their three-dimensional and hydrophilic structure (Ibrahim et al. 2018; Toledo et al. 2019; Ilgin et al. 2019b; Santoso et al. 2019). Generally, hydrogels with stimuli-responsive features act by swelling or shrinking in response to a variety of effects like pH, ionic strength, light, magnetic field or electrical field, and solvents (Thakur and Arotiba 2018; Sahiner et al. 2011; Mahmoud et al. 2014).

In the literature, there are many hydrogels used as adsorbent material. The common feature is preparation as copolymers or hybrids depending on the target molecule for their area of use. Hydrogels may be designed as composites or may include all features of the chemistry of many polymers within their structure, and can be used as unrivaled adsorbent material (Pavithra et al. 2019; Mohammadian et al. 2019; Shen et al. 2019; Zhu et al. 2017; Kaur and Jindal 2018). Acrylic acid, used to increase the water retention capacity during modification of hydrogels, is a pH sensitive anionic monomer with polyelectrolyte carboxyl groups (Janićijević et al. 2019; Dai and Huang 2017; Chen and Sun 2019; Nath et al. 2019). Additionally, due to the ion exchange capability of the cationic monomer 3-(acrylamidopropyl) trimethyl ammonium chloride, different researchers have used it with the aim of developing adsorbent material (Javed et al. 2018; Ghorbanloo et al. 2019). Synthetic hydrogels generally do not have biodegradable structures. As a result, adding a natural polymer to the hydrogel network ensures the adsorbent gains biodegradable and biocompatible structure. Many natural polymers are very cheap, have high adsorbent capacity and are nontoxic. One of the world's richest bioresources, starch is an eco-friendly, naturally occurring and renewable polysaccharide. Thanks to the hydroxyl groups in its structural unit which can promote various functional groups, the chemical modification of its surface is easily achieved, which extends the application range of starch. Hydroxyethyl starch includes all these features and is an important polymer that has not been studied much in the literature (Jiang et al. 2003; Gao et al. 2015; Kenawy et al. 2014). Guo et al. synthesized a crosslinked cationic starch adsorbent from corn starch, with 3-chloro-2-hydroxypropyl trimethylammonium chloride as a cationic etherification agent and epichlorohydrin as a crosslinked agent. Crosslinked cationic starch was used for removal of Reactive golden yellow SNE dye and and its maximum adsorption capacity was found as 308.15 K (Guo et al. 2019). Sharma et al. (2017) prepared starch/poly(alginic acid-cl-acrylamide) nano hydrogel as an effective adsorbent for removing the coomassie bright blue R-250 dye from an aqueous solution. The maximum adsorption capacity was found to be 31.24 mg/g.

In this study, HES-based ionic and non-ionic hydrogels were prepared for the selective adsorption and separation of dyes which are similar organic compounds commonly used in a wide range of fields such as textile, printing and research laboratories. To the best of the authors' knowledge, there are no published studies investigating selective dye adsorption using both ionic and nonionic polymer derivatives based on HES-based polymer. One-step and one-pot methods were employed for the fabrication of hydrogels. The aim of this study is to improve the well-known natural biological properties of HES by modifying it with the addition of synthetic hydrophilic monomers AAc, AAm or APTMAC. The structural, morphologic and swelling properties of the prepared superabsorbent HES/p(NaAAc), HES/p(APTMACl) and HES/p(AAm) hydrogels were investigated. The adsorption isotherms and kinetic parameters for MO and MV dyes were determined for all HES-based hydrogels. Appropriate hydrogels were used to separate a mixture formed of both basic and acid model

dyes. Additionally, effectiveness as an adsorbent for the expulsion of dyes from aqueous media was examined using acid dyes, e.g., bromothymol blue (BB) and methyl orange (MO) and basic dyes, e.g., methyl violet (MV), neutral red (NR), and methylene blue (MB). Due to the simplicity and rapidity of polymerization reactions under mild conditions, HES-based hydrogels developed in this study are suitable for the removal of a wide range of colored organic compounds from water.

Experimental

Materials

Hydroxyethyl starch (HES) (medium MW), acrylamide (AAm, 99%) (3-acrylamidopropyl)trimethylammonium chloride solution (APTMACI, 75%), and acrylic acid (AAc, 99%) used as monomers for the synthesis of hydrogels were purchased from Sigma-Aldrich chemical company and were used without purification. N,N′-methylenebisacrylamide (MBA) as crosslinker, ammonium persulfate (APS) as initiator, N,N,N′,N′-tetramethylethylenediamine (TEMED) as accelerator and all other chemicals were obtained from Sigma-Aldrich chemical company. Bromothymol blue (BB), methyl violet (MV), methyl orange (MO), neutral red (NR) and methylene blue (MB) were used as the source of dyes in adsorption studies. All solutions were prepared with deionized water for hydrogel synthesis and water absorption and dye adsorption studies.

Preparation of hydroxyethyl starch-based hydrogels

HES-based hydrogel films were synthesized with the redox polymerization technique. For synthesis of each hydrogel, HES and monomers with amounts shown in Table 1 were dissolved in water or water/NaOH (containing NaOH with molar equivalent to AAc) solutions. Later crosslinker (MBA) and accelerator (TEMED) were added to the reaction mixture. The reaction mixture was homogenized and 100 μL initiator dissolved in deionized water was added, and polymerization and crosslinking occurred at the same time. At the end of the reaction, hydrogels were washed with 3 × 100 mL deionized water to clean unreacted species (monomer, crosslinker, initiator) for 24 h and then were cut to 5 × 5 mm sizes. After drying in an oven at 50 °C, the hydrogels were stored in a desiccator until characterization and use in adsorption experiments.

Characterization of hydrogels

FT-IR spectra of hydrogels were recorded using an ATR apparatus with a Perkin Elmer FT-IR spectrophotometer. SEM images of hydrogels dried with the freeze dryer method were recorded with JEOL 7100-EDX. The thermal analysis (TGA) of the hydrogels was carried out with a SEIKO SII (TG/DTA 7200) thermal analyzer.

Swelling studies of hydrogels were evaluated in distilled water (DW) and solutions with pH varying from 2 to 10. The swelling capacity of the hydrogels (S, g_{water}/g_{gel}) was evaluated at specified times, and determined with Eq. 1.

$$S_t = \frac{(M_t - M_0)}{M_0} \quad (1)$$

where M_0 and M_t are the mass of the hydrogel before and after the swelling process at time t.

Using the dried weight, the gel percentage of the hydrogels was determined with Eq. 2.

$$\text{Gel}\,\% = \frac{M_2}{M_1} \times 100 \quad (2)$$

Table 1 Synthesis composition of hydrogels

Hydrogel	HES (g)	AAm (g)	APTMACl (g)	AAc (g)	Temed μL	MBA (g)	H_2O (mL)	Rxn time (s)	Gel%
HES/p(APTMACl)	1	–	1	–	200	0.02	2	35	89
HES/p(NaAAc)	1	–	–	1	50	0.02	2	20	80
HES/p(AAm)	1	1	–	–	12.5	0.02	2	10	86

where M_1 and M_2 are the mass of the hydrogels before and after extraction of water, respectively (Erdem et al. 2017).

Adsorption studies

The adsorption properties of hydrogels from aqueous dye solutions with pH 5.6 ± 0.2 were examined using the batch method at ambient temperature (25 °C) for 24 h. Equilibrium adsorption studies for the feed studies were executed by adding known dry weight of hydrogels (~ 20 mg) into 20 mL of dye solution with a concentration range of 25 to 300 mg/L. The dye initial concentration, hydrogel weight and dye solution volume were chosen as 25 mg/L, 20 mg and 100 mL for the time studies, respectively. The dye initial concentration, hydrogel weight and dye solution volume were chosen as 300 mg/L, 20 mg and 20 mL for the temperature studies, respectively. The dye initial concentration, hydrogel weight and dye solution volume were chosen as 300 mg/L, 20 mg and 20 mL for the pH studies, respectively. The equilibrium concentrations of dye were determined with UV–Vis spectrophotometry at λ_{max}: 432, 586, 465, 526, and 660 nm for BB, MV, MO, NR, and MB, respectively. The adsorption capacity of the hydrogel (q, mg of dye per g of gel) at equilibrium (q_e,) and removal percentage (R%) were determined using Eqs. 3a and 3b.

$$q_e = (C_0 - C_e)V/W \tag{3a}$$

$$R\,\% = (C_0 - C_e)/C_0 \times 100 \tag{3b}$$

where C_0, and C_e, are dye concentration before and after the adsorption process at time t, respectively, V is the volume of the dye solution (L), and W is the mass of the dry gel (g).

Results and discussion

Preparation and characterization of hydroxyethyl starch-based hydrogels

The most important feature of polymer structures is that they can be designed according to area of application. Polymers, which can be prepared as both copolymer and composite, contain many features in their structure. Polymers to be designed for environmental applications should not dissolve in the presence of solvents, be cheap, have repeated use, be flexible and at the same time mechanically resistant. In addition to the polymeric structure being insoluble, the main condition for displaying the mechanically desired features is preparation with a crosslinker. Polymer adsorbents that can house all these features within their structure at the same time are unrivaled engineering wonders. As a result, hydrogels lead the list of polymeric structures chosen as molecular adsorbents. The greater the water-absorbing ability of these hydrogels to be used as adsorbents in aqueous media, the greater the adsorption capacity for organic or inorganic pollutants from aqueous media. Inclusion of monomers with ionic character in hydrogel structures increases the hydrogel's water and ion retention capacities. Hydrogels prepared with both anionic and cationic character can be used for adsorption of all ions from water, and also with the aim of separating these species. AAc and APTMACI are ionic monomers. In the literature, they are used for preparation of many adsorbents. Within the scope of this study, the main aim in selecting both anionic and cationic monomers was preparation of a serial adsorbent hydrogel for waste dyes created as a result of a variety of industrial activities. The HES structure contains many -OH groups. At the same time, organic molecules have the potential to form hydrogen bonds. As a result, hydrogels containing HES, which is natural polymer, can have improved mechanical and water retention features.

With the aim of adsorption and separation of organic dyes from aqueous media, HES/p(NaAAc), HES/p(APTMACl) and HES/p(AAm) ionic and neutral hydrogels were prepared as given in Table 1. In the literature, generally 1–12 h is expected as reaction time for hydrogel synthesis. However, the inclusion of HES in the hydrogel structure reduced the reaction time to 10–35 s, as given in Table 1. This means hydrogel synthesis will have very cheap cost for industrial applications. Also, the gel percentage of the prepared hydrogels is given in Table 1. The scheme for synthesis reactions and structures of hydrogels are given in Fig. 1. The most important function in preparation of interpenetrating network (IPN) hydrogels is the development of hydrogel features with a network structure. Here ionic monomers increase the water retention and adsorption

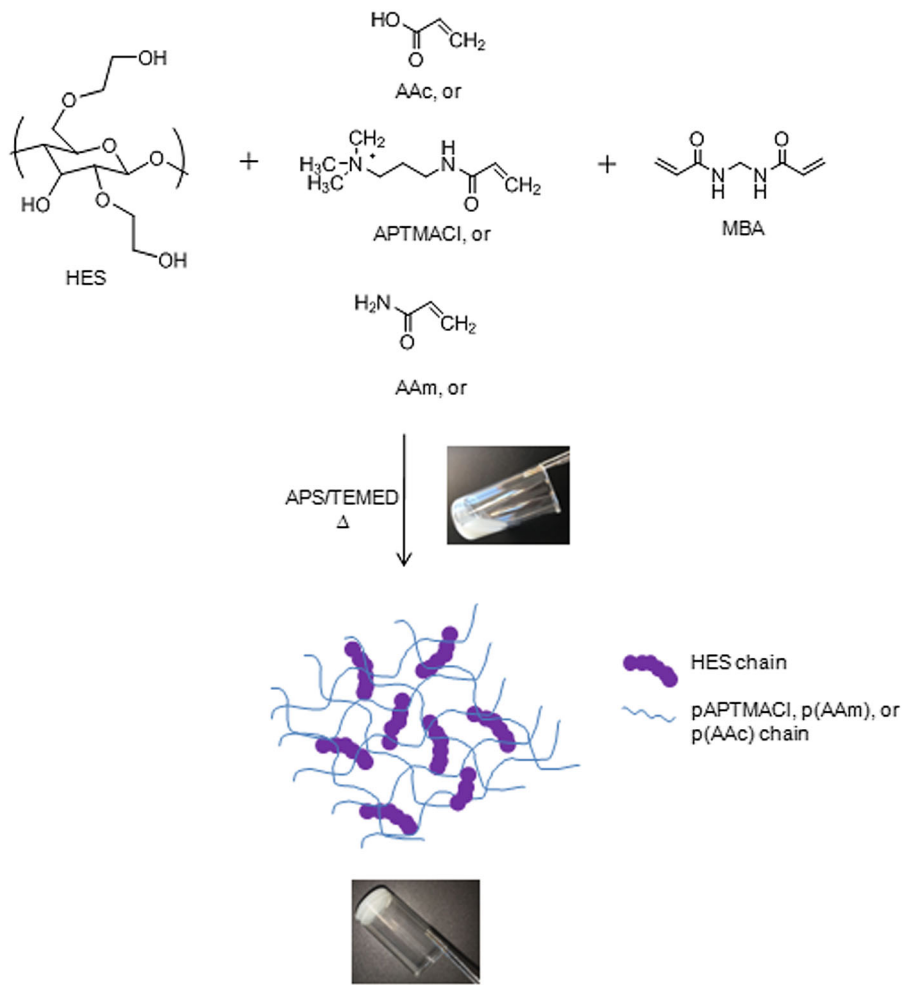

Fig. 1 Synthesis scheme for HES-based hydrogels

capacities of hydrogels, while natural polymers like HES add flexibility and stability to the hydrogel structure. At the same time, the -OH groups support the hydrophilic structure.

SEM images of HES particles with 8-10 µm size are given in Fig. 2a, b. Here, the homogeneity of HES particles appears to be high. SEM images were recorded for characterization of the morphologic structure and porosity of the synthesized hydrogels. To prevent collapse of the porous structure of the hydrogels during drying, water-absorbed hydrogels were frozen at − 20 °C. Hydrogels were later dried in a freeze dryer. The SEM images of hydrogels are given in Fig. 2c–h. As seen in Fig. 2c–h, HES-based hydrogels have homogeneous distribution of HES in their structures. AAc, APTMACI and AAm are hydrophilic monomers. Each of the three monomers ensures porosity in the hydrophilic-character hydrogels. As seen in Fig. 2c–h, HES/p(NaAAc), HES/p(APTMACl) and HES/p(AAm) hydrogels have nearly 10-40 µm pore dimensions. Both pore sizes and hydrophilic features of monomers in the structure show these hydrogels are each unrivaled adsorbent materials for use in aqueous media.

As shown in Fig. 3, the FTIR spectra of HES has a wide band at 3312 cm^{-1} and another at 1639 cm^{-1} which belong to the stretching and in-plane vibrations of O–H, respectively; bands at 2924 cm^{-1} correspond to C–H stretching; and a strong and complex band at 1155, 1077, and 998 cm^{-1} is due to C–O bond stretching (Silva et al. 2014). In addition to the characteristic peaks of HES, the distinctive peaks of

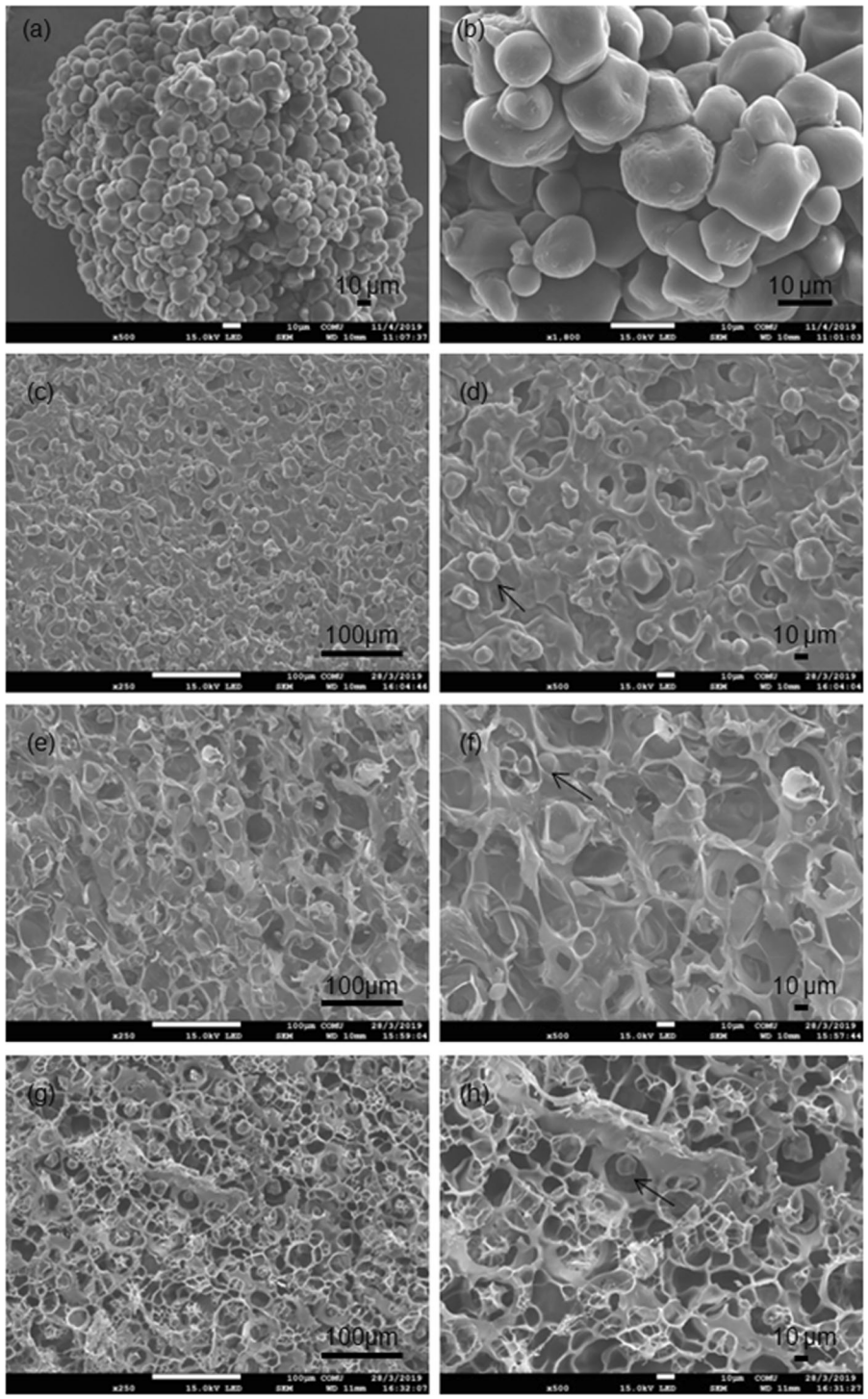

Fig. 2 SEM image of **a** and **b** HES, **c** and **d** HES/p(APTMACl), **e** and **f** HES/p(NaAAc), **g** and **h** HES/p(HEMA) hydrogels at different magnifications

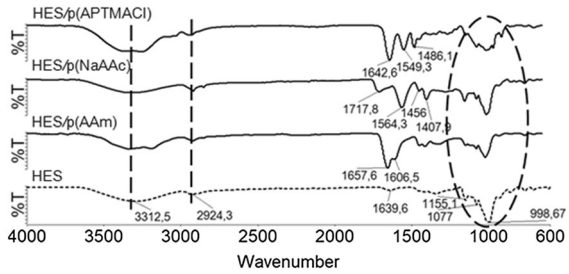

Fig. 3 FTIR spectra of HES-based hydrogels

blend polymers are listed as follows. The most striking peak of HES/p(APTMACl) was observed at 1486 cm^{-1}, which corresponds to C-H symmetric bending of the methyl groups on the quaternary ammonium (Yang et al. 2010). The absorption bands at 1642 and 1549 cm^{-1} displayed by the amides are due to C=O and N–H stretching vibrations. The very intense characteristic band of HES/p(NaAAc) at 1564 cm^{-1} is due to C=O asymmetric stretching in the carboxylate anion that is confirmed by peaks at 1456 and 1407 cm^{-1} which are related to the symmetric stretching mode of the carboxylate anion (Bao et al. 2011). The presence of a weak band at 1717 cm^{-1} indicates a small fraction of the carboxylic acid group was not totally neutralized in the first step of synthesis. The absorption bands for HES/p(AAm) at 1657 and 1606 cm^{-1} displayed by the amides are due to C=O and N–H stretching vibrations. These observations show that all hydrogels were successfully prepared.

TG analysis was performed to predict their thermal stability up to a temperature of 600 °C from a temperature of 30 °C with the heating rate at 10 °C.min^{-1} in a nitrogen atmosphere. The TGA curves for HES, HES/p(NaAAc), HES/p(APTMACl) and HES/p(AAm) are shown in Fig. 4. In the first stage between 30 and 150 °C, the bound water in the structure of the materials was removed. The main degradation of HES occurred in the second stage between 285 and 396 °C which shows the breakage of long chains of starch and destruction of the glucose rings (Ismail et al. 2017). The two-stage degradation step indicated by all hydrogel samples was between 275 and 600 °C. The decomposition percentages and temperatures for HES/p(NaAAc), HES/p(APTMAC1) and HES/p(AAm) hydrogels are as follows; 34% for 250–430 °C and 19% for 430–500 °C; 46% for 250–310 °C and 23% for 310–450 °C; and 31% for

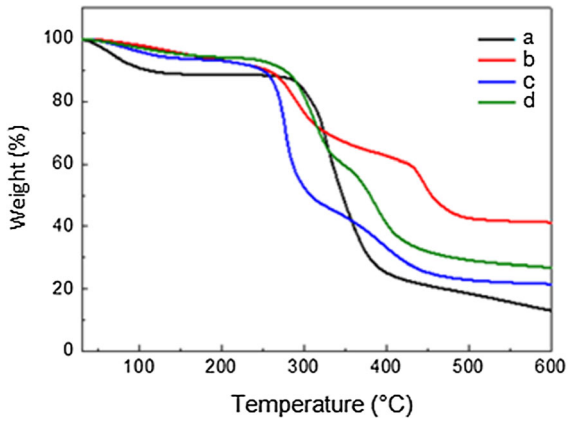

Fig. 4 TGA spectra of HES-based hydrogels, **a** HES, **b** HES/p(NaAAc), **c** HES/p(APTMACl) and **d** HES/p(AAm)

250–340 °C and 36% for 340–425 °C, respectively. In anionic, cationic and neutral character hydrogels, the structure of the starch was degraded first and then the homopolymer was degraded. Thus, it was observed that monomers with anionic, cationic and neutral characters were incorporated into the HES structure and hydrogels were synthesized successfully.

The water retention capacity of hydrogels to be used for adsorption of organic or inorganic species in aqueous media allows their classification as good adsorbent material. Within the scope of the study, HES/p(NaAAc), HES/p(APTMACl) and HES/p(AAm) hydrogels synthesized with anionic, cationic and neutral character each have hydrophilic structures. The dynamic swelling and pH swelling behavior of hydrogels is given in Fig. 5. The –COONa group in the structure of HES/p(NaAAc) hydrogel and the $N^{+-}(CH_3)_3Cl^-$ group in the structure of HES/p(APTMACl) hydrogel increase the water retention capacity of the hydrogels due to their ionization properties. Additionally, ionized functional groups within the network structure repel each other, contributing to opening of the network and pores. This causes more water retention in HES/p(AAm) hydrogel with ionic character. As seen in Fig. 5a, HES/p(APTMACl), HES/p(NaAAc) and HES/p(AAm) hydrogels have equilibrium water retention values, reached in nearly 200 min, of 40.06 g/g, 20.67 g/g and 2.47 g/g, respectively.

Swelling behavior at a variety of pH values displays similar behavior to adsorbable organic or inorganic pollutant amounts for hydrogels to be used as

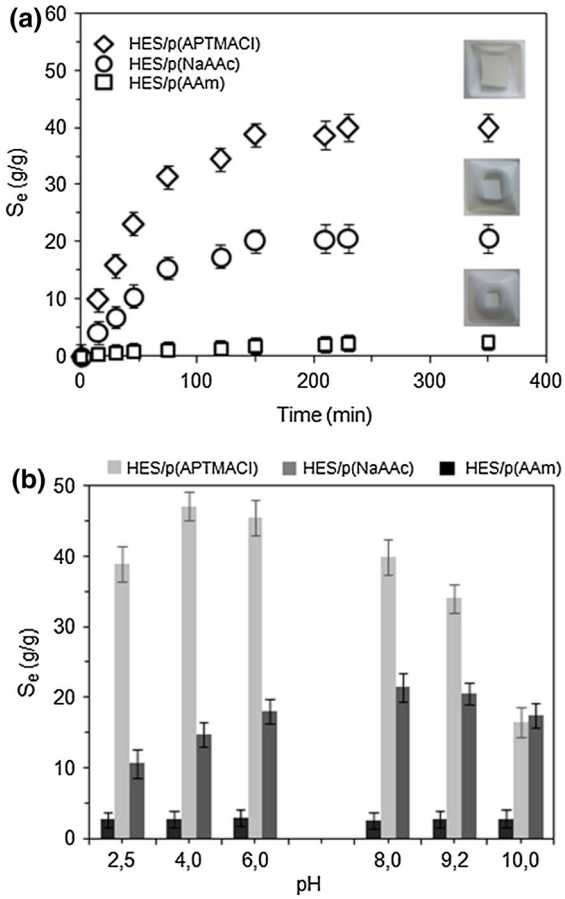

Fig. 5 Effect of **a** time, and **b** pH on swelling ratio of HES-based hydrogels

adsorbent material. Figure 5b gives the water absorption behavior of hydrogels at a variety of pH values. The $–COO^-$ group in the sodium acrylate structure and the –OH groups in the HES structure form intermolecular hydrogen bonds at pH < 6. This reduces the entry of water into the structure. At higher pH values, breaking of these hydrogen bonds increases the water retention capacity of the hydrogel. In high pH environments (pH > 7), the increasing presence of OH^- ions interacts electrostatically with the cationic group in the hydrogel structure preventing water from entering the network structure. This lowers the water absorption capacity of the hydrogel. At low pH values, H^+ ions in the aqueous medium ensure electrostatic repulsive forces and expand the hydrogel network structure. This increases the water absorption capacity of HES/p(APTMACl) hydrogel. The HES/p(AAm) hydrogel with no ionic groups is not pH sensitive. Hydrophilic –OH and $–NH_2$ groups in the structure do not change the water retention capacity of hydrogels at various pH values. Accordingly, on Fig. 5b, the maximum water retention capacity of HES/p(NaAAc) hydrogel is 21.34 g/g at pH = 8, and this value is greater than the water retention capacity of HES/p(AAm). As seen in Fig. 5b, maximum water absorption capacity for HES/p(APTMACl) hydrogel is 47.10 g/g at pH = 4. Also, all hydrogels remained stable in varying pH environments.

Adsorption of dye materials with HES-based hydrogels

The effect of dye concentration on the adsorption of MO and MV from aqueous media by HES/p(NaAAc), HES/p(APTMACl) and HES/p(AAm) hydrogels was determined at 7 different concentrations in the interval from 0 to 300 mg/L. The results obtained from studies with 20 mL dye solution and 20 mg adsorbent hydrogel are given in Fig. 6a. Accordingly, cationic HES/p(APTMACl) hydrogel had maximum adsorption capacity of 220 mg/g for the anionic dye MO (300 mg/L initial concentration). Additionally, HES/p(NaAAc) hydrogel containing anionic functional groups had maximum adsorption capacity of 175 mg/g for the cationic dye of MV. Figure 6a gives the maximum MV adsorption amounts for HES/p(AAm) and HES/p(APTMACl) hydrogels as 7.95 mg/g and 3.58 mg/g. Similarly, for MO dye, maximum adsorption values obtained with HES/p(AAm) and HES/p(NaAAc) hydrogels were 2.91 mg/g and 2.46 mg/g. Here, especially electrostatic interactions between HES/p(NaAAc) as anionic hydrogel and MV as cationic dye and between HES/p(APTMACl) as cationic hydrogel and MO as anionic dye were considered the main factors as the mechanism of adsorption during the dye adsorption process in our study. In addition to secondary interactions between all hydrogels and dyes, such as hydrogen bonds and van der Waals forces, good absorption capability of a plurality of porous networks permitting capture of dye molecules is also included in the adsorption mechanism. Figure 6b gives the maximum adsorption amounts for dye adsorption using 20 mg hydrogel and 25 mg/L concentration dye solution. According to the figure, adsorption equilibrium for ionic hydrogels is reached in nearly 24 h.

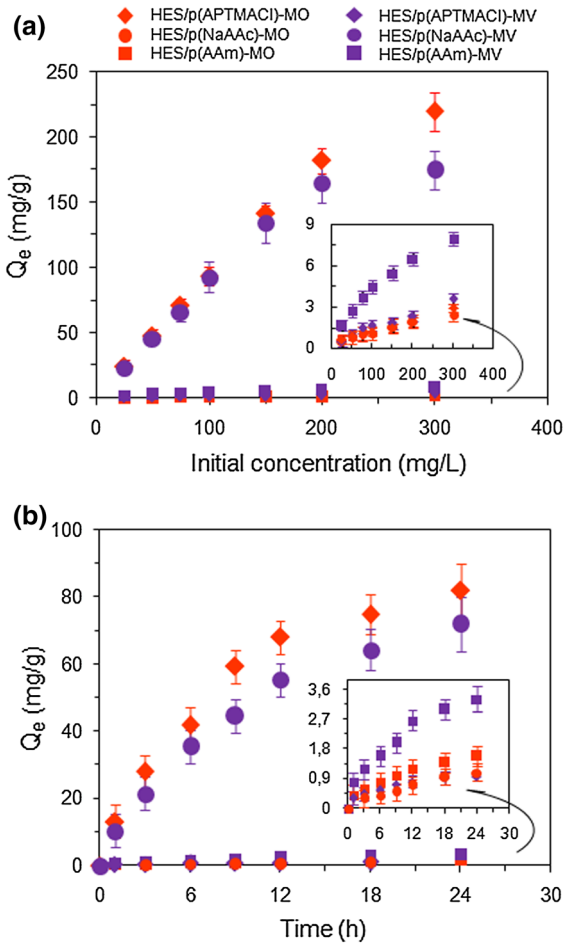

Fig. 6 Effect of **a** initial feed concentration and **b** time for the adsorption of dyes by the hydrogel

The equilibrium adsorption isotherm for dye molecules explains the interaction between adsorbent and organic dye. Additionally, it provides important information about the mechanism of the adsorption process and optimization. The equilibrium adsorption isotherm for MV and MO adsorption by HES/p(NaAAc), HES/p(AAm) and HES/p(APTMACl) hydrogels were investigated with the Langmuir (Eq. 4) and Freundlich (Eq. 5) models (Langmuir 1918; Freundlich 1906).

$$\frac{1}{q_e} = \frac{1}{K_L q_m C_e} + \frac{1}{q_m} \tag{4}$$

$$\log q_e = \log K_F + \frac{\log C_e}{n} \tag{5}$$

where q_m, C_e, K_L, K_F and n are the maximum adsorption capacity (mg/g), the equilibrium concentration (mg/L), Langmuir constant, Freundlich adsorption capacity and Freundlich constant, respectively. For the Langmuir isotherm, the graph of $1/q_e$ against $1/C_e$ was drawn with experimental results and based on the above equation, q_m and K_L values were calculated. For the Freundlich isotherm, the graph of $\log q_e$ against $\log C_e$ was drawn with experimental results and n and K_F values were calculated from the above equation (Chakraborty et al. 2019).

Adsorption equilibrium studies provide important information about the maximum adsorption capacity of an adsorbent and its affinity for different dye molecules. The Langmuir isotherm model suggests that this adsorption is better described as monolayer adsorption with uniform energies. The Freundlich model suggests that this adsorption is better described as multilayer adsorption processes on a heterogeneous adsorbent surface where the adsorption heat and adsorption affinity are not evenly distributed.

Table 2 shows the q_{max} and K_L values for the Langmuir isotherm, the K_f and n values for the Freundlich isotherm and the regression coefficients (R^2) for both isotherms. In addition to the correlation coefficient, the fit of an isotherm model to experimental data and calculated maximum q_e values can be evaluated by comparison with experimental data. When the correlation coefficients (R^2) and maximum q_e values are calculated for adsorption of dye by hydrogels, they fit the Langmuir and Freundlich isotherms; however, there appears to be better fit to the Langmuir isotherm model. The $R_L(= 1/(1 + K_L C_0)$ value, showing whether the adsorption in the Langmuir isotherm model is favorable or not, was between 0 and 1 for all hydrogels and dyes in Table 2, so adsorption is favorable ($0 < R_L < 1$). For the Freundlich isotherm model, the adsorption capacity (K_F) and heterogeneity factor (1/n) were calculated. The 1/n value is between 0 and 1. The closer the 1/n factor is to 0, the more heterogeneous the surface. The 1/n value being smaller than 1 in Table 2 indicates all hydrogels are suitable for the removal of MO and MV dyes.

With the aim of investigating the adsorption and potential rate control steps in the mechanism to aid in selecting the best study conditions, many models have been used in the literature to quantitatively define the

Table 2 Isotherms and kinetic parameters for hydrogels

Isotherms/kinetic parameters	MV			MO		
	HES/p(APTMACl)	HES/p(NaAAc)	HES/p(AAm)	HES/p(APTMACl)	HES/p(NaAAc)	HES/p(AAm)
q_{exp}	3.58	175.0	7.96	220.0	2.47	2.92
Langmuir						
q_{max} (mg/g)	6.62	185.2	9.17	238.1	2.84	3.33
K_L(L/mg)	3.39×10^{-3}	1.14×10^{-1}	1.44×10^{-1}	9.1×10^{-2}	8.72×10^{-3}	7.19×10^{-3}
R_L	0.92–0.49	0.26–0.028	0.22–0.23	0.31–0.035	0.82–0.28	0.85–0.32
R^2	0.987	0.968	0.989	0.995	0.980	0.888
Freundlich						
K_F (mg/g)	0.074	25.4	0.36	32.5	0.066	0.059
1/n	0.682	0.476	0.584	0.519	0.641	0.680
R^2	0.995	0.839	0.992	0.893	0.991	0.948
q_{exp} (mg/g)	0.965	72.1	3.32	82.2	1.13	1.62
Pseudo-first-order						
q_{max} (mg/g)	0.78	74.44	3.23	75.64	1.30	1.42
$K_1(h^{-1})$	0.160	0.123	0.124	0.139	0.113	0.105
R^2	0.981	0.992	0.969	0.994	0.932	0.990
Pseudo-second-order						
q_{max} (mg/g)	1.16	80.64	2.79	100	1.28	1.33
K_2[g/(mg.h)]	0.156	1.78×10^{-3}	0.135	1.49×10^{-3}	0.073	0.302
R^2	0.974	0.991	0.913	0.992	0.923	0.923

kinetic behavior of adsorption processes by hydrogels. The most commonly used are the pseudo first-order (Eq. 6) and pseudo second-order (Eq. 7) adsorption models.

The pseudo-first-order equation of Lagergren (1898) analyzes the adsorption of a liquid/solid system based on the solid capacity, while the pseudo-second-order equation of Ho and McKay (1999) analyzes the amount of sorbate adsorbed onto a sorbent based on solid phase sorption.

$$\ln(q_e - q_t) = \ln q_e - K_1 t \tag{6}$$

$$\frac{1}{q_t} = \frac{1}{K_2 q_e^2 t} + \frac{1}{q_e} \tag{7}$$

where q_e, q_t, t, K_1 and K_2 are the equilibrium adsorption capacity (mg/g), the adsorption capacity at t time (mg/g), *t* is the contact time (h), and K_1 and K_2 are the first-order rate constant and the second-order rate constant, respectively. For pseudo first-order equation, the graph of $\ln(q_e\text{-}q_t)$ against t was drawn from experimental results and the q_e and K_1 values were calculated based on the equation. For pseudo second-order equation, the graph of $1/q_t$ against 1/t was drawn from experimental results and the q_e - and K_2 values were calculated based on the equation (Liang et al. 2019). The correlation coefficients, q_e (calculated) and q_e (experimental) are given together in Table 2. The correlation coefficients for the pseudo first-order equation are higher than for the pseudo second-order equation. Additionally, the theoretical q_e values are closer to the experimental q_e values. In light of these results, the adsorption system for MV and MO dyes with HES/p(NaAAc), HES/p(AAm) and HES/p(APTMACI) hydrogels was concluded to follow a pseudo first-order model. Accordingly, adsorption is controlled by electrostatic interaction between dye molecules and hydrogels and hydrogel amount significantly affects the adsorption rate.

In order to determine the thermodynamic nature of the adsorption process, the adsorption amounts were investigated at various temperatures such as 25, 40 and 55 °C. For this purpose, MO and HES/p(APTMACI),

and MV and HES/p(NaAAc) were selected as dyes and hydrogels, where the strong electrostatic interaction between the dye and the adsorbent was dominant. The effect of the temperature of the solution on adsorption of dyes by hydrogels is shown in Fig. 7a. It can be seen from the figure that the adsorption capacity increases with increasing temperature.

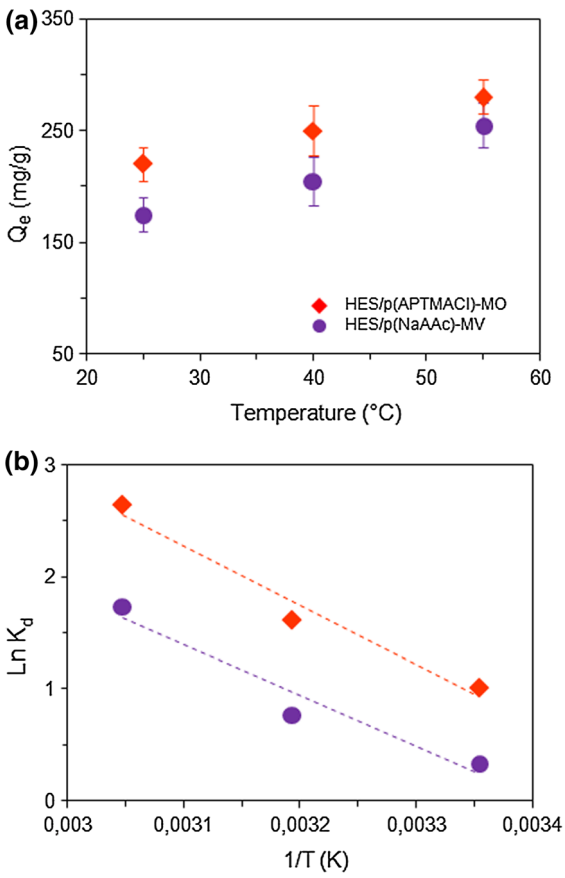

Fig. 7 **a** Effect of temperature on the adsorption of dyes by the hydrogels, **b** plot of lnKd versus 1/T for adsorption of dyes

Thermodynamic parameters such as Gibbs free energy (ΔG, kJ/mol), enthalpy (ΔH, kJ/mol) and entropy (ΔS, kJ/mol.K) were calculated from Eq. 8 and are shown in Table 3 (Ngwabebhoh et al. 2019). The values of ΔH and ΔS were calculated by plotting $\ln K_d$ against 1/T (K) according to Fig. 7b.

$$K_d = (C_s)/C_e \tag{8a}$$

$$\ln K_d = \frac{-\Delta H^\circ}{RT} + \frac{\Delta S^\circ}{R} \tag{8b}$$

$$\Delta G^\circ = -RT\ln K_d \tag{8c}$$

$$\Delta G^\circ = \Delta H^\circ - T\Delta S^\circ \tag{8d}$$

where C_e is equilibrium concentration in dye solution (mg/L), C_s is the adsorbed concentration of dye in dye solution (mg/L), T is the temperature (K) and R is the gas constant [8.314 J/(mol.K)].

The thermodynamic evaluation substantiates the endothermic nature of the adsorption process due to the positive value of ΔH°. The positive value for entropy (ΔS°) change illustrates the adsorption occurs at the interface between hydrogel and dye with increased randomness. Negative ΔG° values at all temperatures mean a spontaneous adsorption process, and the decrease in ΔG° with increasing temperature indicates that the adsorption process is more suitable at high temperatures.

Since the pH of the solution can affect the surface charge of the adsorbent and the molecular state of the dye molecules, the adsorption amounts were calculated at various pHs to determine the sensitivity of the adsorption process to the ambient pH. For this purpose, MO and HES/p(APTMACl), and MV and HES/p(NaAAc) were selected as dyes and hydrogels. It was expected that strong electrostatic interaction between the dye and the adsorbent would come to the fore at varying pHs. The effect of the pH of the

Table 3 Thermodynamic parameters for hydrogels

Thermodynamic parameters	HES/p(APTMACl)-MO	HES/p(NaAAc)-MV
ΔG° (kj/mol)		
298.15 K	− 2.29	− 0.60
313.15 K	− 4.62	− 2.53
328.15 K	− 6.95	− 4.45
ΔH° (kj/mol)	43.90	37.64
ΔS° [kj/(mol K)]	0.15	0.13
R^2	0.968	0.941

solution on the adsorption of dyes by hydrogels is shown in Fig. 8. Adsorption of methyl orange by HES/p(APTMACI) is due to the electrostatic attraction between the cations in the adsorbent and the anions in the dye. At low pH (2.0), the structure of the methyl orange changes to its cationic form (Qi et al. 2018). This results in significantly limited equilibrium adsorption capacity. The adsorption capacity of MO increased significantly in the pH range from 2.0 to 6.0, but no significant change was observed after pH 6.0. It is clear that the removal of MV from Fig. 8 increases with the pH increase from 2 to 6 and is constant beyond pH 6. This cationic dye exhibits a nearly similar tendency to methyl orange for dye adsorption at various pHs, i.e. it shows high adsorption in the high pH range after pH 6. Below pH 4, dye adsorption decreases due to the conversion of carboxylic groups in hydrogels to carboxylic acid (Thakur and Arotiba 2018). The ionization of carboxylic acid groups above pH 6 can increase the negative charge on the adsorbent surface, which increases the amount of MV dye adsorption in the basic medium. This caused strong electrostatic interactions between the carboxylate groups in the hydrogel and the positively-charged tertiary amine groups in MV. As understood from the pH results, all experiments were performed in aqueous

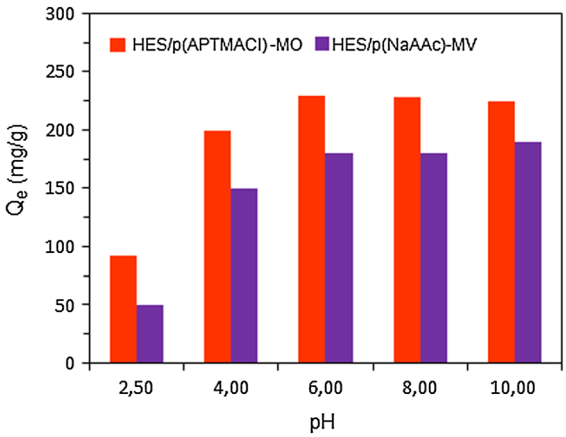

Fig. 8 Effect of pH on the adsorption of dyes by the hydrogels

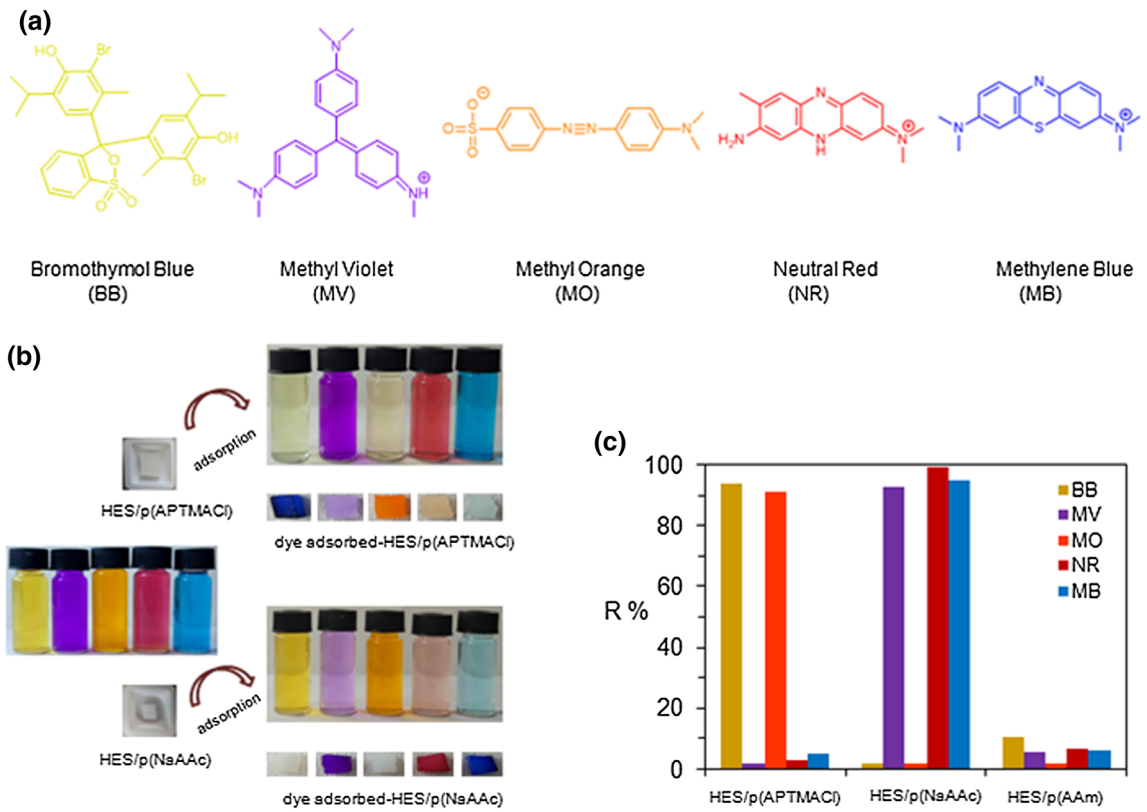

Fig. 9 **a** Chemical structures of dyes used, **b** digital images before and after dye adsorption studies using HES/p(APTMACI) and HES/p(NaAAc), and **c** removal % of dyes by hydrogels

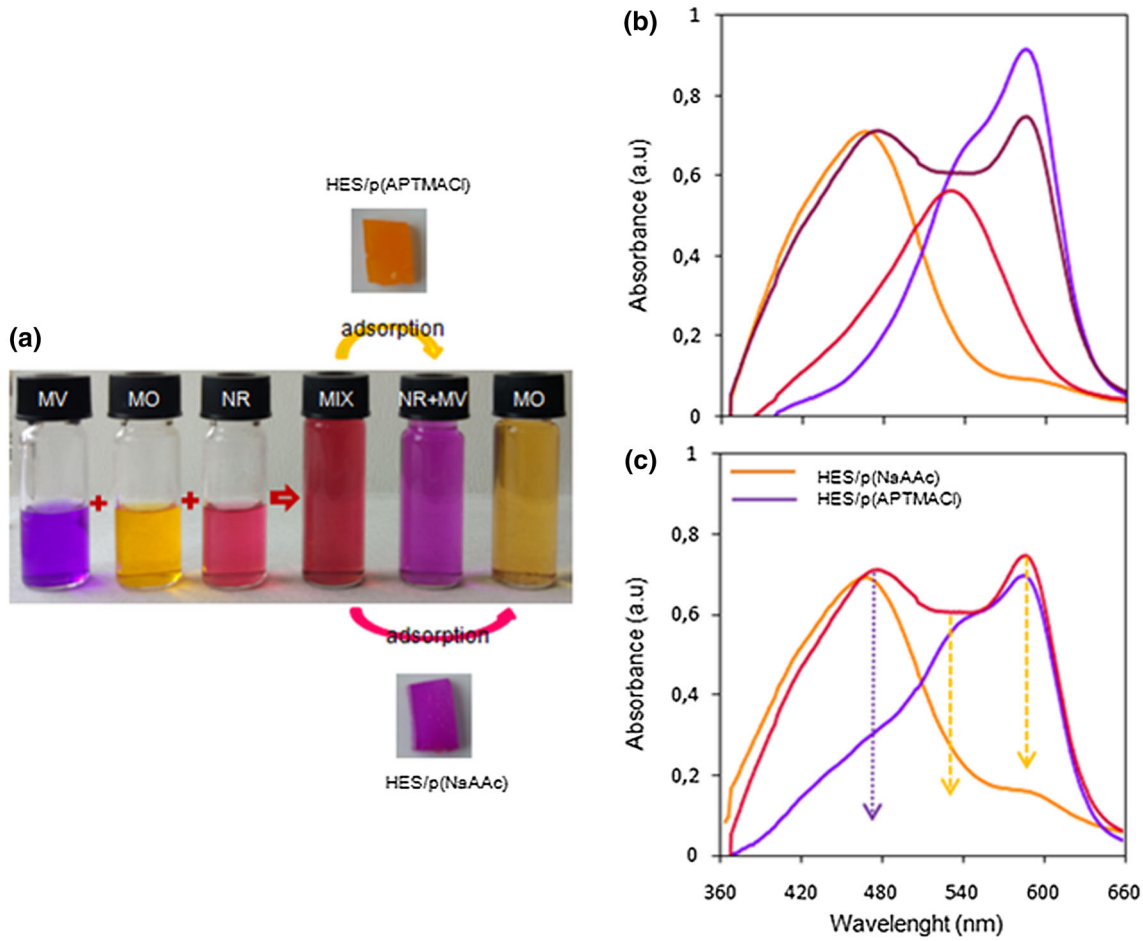

Fig. 10 **a** Digital images of the dye mixture of MV/MO/NR before and after adsorption by hydrogels, and adsorption spectra **b** before and **c** after dye adsorption by hydrogels

dyes solutions at pH 5.6, which is close to their natural pH, since no significant increase in adsorption capacity was observed in extremely acidic or extremely basic environments.

The dyes BB, MV, MO, NR and MB with ionic character, with molecular formulas given in Fig. 9a, can also be adsorbed from aqueous solutions by HES/p(NaAAc) and HES/p(APTMAC1) (20 mg) hydrogels with ionic character. As seen in Fig. 9b, MV, NR and MB solutions in 100 mg/L (20 mL) dye solution can be cleaned with HES/p(NaAAc) hydrogel. Again, using HES/p(APTMACl) hydrogel, 100 mg/L (20 mL) anionic BB and MO solutions can be cleaned with high efficiency. The dye initial concentration, hydrogel weight and dye solution volume were chosen as 100 mg/L, 20 mg and 20 mL for the various dye studies at 25 °C in 24 h respectively. The maximum adsorption amounts for all dye materials are given in Fig. 9c.

Accordingly, BB and MO adsorption with HES/p(APTMACl) hydrogel was completed with 94% and 91.2% efficiency. Again, with 100 mg/L (20 mL) concentration, HES/p(NaAAc) hydrogel removed MV, NR and MB dyes with 93%, 99% and 95% efficiency, respectively.

As a result of industrial activities, a variety of dye mixtures may be created as waste. It is very important that waste in the form of these types of mixtures be cleaned with maximum efficiency and selectivity by hydrogels with appropriate structure. Figure 10a shows a solution mixture of MV, MO and NR with 25 mg/L concentration that do not interact with each other. Here, to selectively separate the dye mixture, there is a need for both cationic and anionic hydrogels.

Table 4 Comparison of MO/MV adsorption capacity of some hydrogels discussed in the literature

Hydrogel adsorbent	MO Q_{max} (mg/g)	MV Q_{max} (mg/g)	References
HPEI-MBA	1552.76	–	Zhu et al. (2019)
Alginate-coated perlite beads	–	149.2	Parlayici (2019)
Poly(PEGM-co-DEAEM)	212.7	–	Alokour and Yilmaz (2019)
KG-cl-poly(AA-co-NVI)	–	286.01	Jana et al. (2018b)
Banana pseudo-stem-g-p(NaAC-co-AM)	124	–	Bello et al. (2018)
SA-g-PAA/TiO_2	–	1156.61	Thakur and Arotiba (2018)
XG-cl-pAA/rGO	–	1052.63	Makhado et al. (2018)
p(AA-co-AMPS)-kaolin	506	–	Tang et al. (2018)
Core@shell PAA microgels/PES beads	2.29	43.37	Chen et al. (2017)
PC-g-(SA-co-NIPA)	–	265.49	Singha et al. (2017)
GG-g-poly(DMAEMA))	25.8	–	Karthika and Vishalakshi (2015)
HES/p(APTMACl)	238.1	6.62	This work
HES/p(NaAAc)	2.84	185.2	This work
HES/p(AAm)	3.33	9.17	This work

As seen in Fig. 10a, the cationic HES/p(APTMACl) hydrogel cleaned the majority of MO from the mixture. Again, the anionic HES/p(NaAAc) hydrogel removed MV and NR from the medium with selective adsorption. Figure 10b, c gives the UV–VIS spectra before and after adsorption for the dye mixture. When the spectra are investigated, the peak for NR in the medium is completely lost after adsorption, with the MO and MV concentrations significantly reduced.

In the literature, a variety of adsorbent materials were used for MO and MV dyes and the maximum adsorption amounts are given in Table 4. Accordingly, the maximum adsorption capacities for MO and MV by HES/p(APTMACl) and HES/p(NaAAc) comply with the literature values.

Conclusion

In conclusion, in this study, we prepared a new adsorbent hydrogel material as a solution to water pollution problems occurring due to the effect of increasing industrialization. HES/p(NaAAc), HES/p(APTMACl) and HES/p(AAm) hydrogels containing HES, which is a natural polymer, were used for adsorption and separation of anionic and/or cationic dyes from aqueous media due to the anionic and cationic groups added to their structure. The adsorbent material removed organic dyes from aqueous media with over 90% efficiency. According to these results, we can say that we have contributed with the addition of new superabsorbent material to the literature. In light of our results, we continue our studies about development of new superabsorbents to ensure adsorption or separation of both groups of dyes.

Compliance with ethical standards

Conflict of interest There is no conflict of interest.

References

Alokour M, Yilmaz E (2019) Photoinitiated synthesis of poly(poly(ethylene glycol)methacrylate-co-diethyl amino ethyl methacrylate) superabsorbent hydrogels for dye adsorption. J Appl Polym Sci 136:47707

Bao Y, Ma J, Li N (2011) Synthesis and swelling behaviors of sodium carboxymethyl cellulose-g-poly(AA-co-AM-co-AMPS)/MMT superabsorbent hydrogel. Carbohydr Polym 84:76–82

Bello K, Sarojini BK, Narayana B, Rao A, Byrappa K (2018) A study on adsorption behavior of newly synthesized banana pseudo-stem derived superabsorbent hydrogels for cationic and anionic dye removal from effluents. Carbohydr Polym 181:605–615

Bhattacharyya R, Ray SK (2014) Enhanced adsorption of synthetic dyes from aqueous solution by a semi-

interpenetrating network hydrogel based on starch. J Ind Eng Chem 20(5):3714–3725
Capanema NSV, Mansur AAP, Mansur HS, de Jesus AC, Carvalho SM, Chages P, de Oliveira LC (2018) Eco-friendly and biocompatible cross-linked carboxymethylcellulose hydrogels as adsorbents for the removal of organic dye pollutants for environmental applications. Environ Technol 39(22):2856–2872
Chakraborty R, Verma R, Asthana A, Vidya SS, Singh AK (2019) Adsorption of hazardous chromium (VI) ions from aqueous solutions using modified sawdust: kinetics, isotherm and thermodynamic modelling. Int J Environ Anal Chem. https://doi.org/10.1080/03067319.2019.1673743
Chen Y, Sun P (2019) pH-Sensitive polyampholyte microgels of poly(acrylic acid-co-vinylamine) as injectable hydrogel for controlled drug release. Polymers 11(2):285
Chen S, Zhang X, Huang H, Zhang M, Nie C, Lu T, Zhao W, Zhao C (2017) Core@shell poly(acrylic acid) microgels/polyethersulfone beads for dye uptake from wastewater. J Environ Chem Eng 5:1732–1743
Dai H, Huang H (2017) Synthesis, characterization and properties of pineapple peel cellulose-g-acrylic acid hydrogel loaded with kaolin and sepia ink. Cellulose 24:69–84
Erdem A, Ngwabebhoh FA, Çetintas S, Bingöl D, Yildiz U (2017) Fabrication and characterization of novel macroporous Jeffamine/diamino hexane cryogelsfor enhanced Cu(II) metal uptake: optimization, isotherms, kinetics and thermodynamic studies. Chem Eng Res Des 117:122–138
Freundlich HMF (1906) Over the adsorption in solution. J Phys Chem 57A:1100–1107
Gao LX, Chen JL, Han XW, Yan SX, Zhang Y, Zhang WQ, Gao ZW (2015) Electro-response characteristic of starch hydrogel crosslinked with Glutaraldehyde. J Biomater Sci Polym Ed 26(9):545–557
Ghorbanloo M, Moharramkhani N, Yazdely TM, Monfared HH (2019) Cationic hydrogel and graphene oxide based cationic hydrogel with embedded palladium nanoparticles in the aerobic oxidation of olefins. J Porous Mater 26(2):433–441
Guo J, Wang J, Zheng G, Jiang X (2019) Optimization of the removal of reactive golden yellow SNE dye by cross-linked cationic starch and its adsorption properties. J Eng Fibers Fabr 14:1–13
Ho YS, McKay G (1999) Pseudo-second order model for sorption processes. Process Biochem 34:451–465
Hu T, Liu Q, Gao T, Dong K, Wei G, Yao J (2018a) Facile preparation of tannic acid-poly(vinyl alcohol)/sodium alginate hydrogel beads for methylene blue removal from simulated solution. ACS Omega 3(7):7523–7531
Hu XS, Liang R, Sun G (2018b) Super-adsorbent hydrogel for removal of methylene blue dye from aqueous solution. J Mater Chem A 6(36):17612–17624
Ibrahim AG, Hai FA, El-Wahab HA, Aboelanin H (2018) Methylene blue removal using a novel hydrogel containing 3-Allyloxy-2-hydroxy-1-propanesulfonic acid sodium salt. Adv Polym Technol 37(8):3561–3573
Ilgin P, Ozay H, Ozay O (2019a) A novel hydrogel containing thioether group as selective support material for preparation of gold nanoparticles: synthesis and catalytic applications. Appl Catal B: Environ 241:415–423
Ilgin P, Ozay H, Ozay O (2019b) A new dual stimuli responsive hydrogel: modeling approaches for the prediction of drug loading and release profile. Eur Polym J 113:244–253
Ismail S, Mansor N, Man Z (2017) A study on thermal behaviour of thermoplastic starch plasticized by [Emim] Ac and by [Emim] Cl. Procedia Eng 184:567–572
Jana S, Pradhan SS, Tripathy T (2018a) Poly(N, N-dimethylacrylamide-co-acrylamide) grafted hydroxyethyl cellulose hydrogel: a useful congo red dye remover. J Polym Environ 26(7):2730–2747
Jana S, Ray J, Mondal B, Pradhan SS, Tripathya T (2018b) pH responsive adsorption/desorption studies of organic dyes from their aqueous solutions by katira gum-cl-poly(acrylic acid-co-N-vinyl imidazole) hydrogel. Colloid Surf A Physicochem Eng Asp 553:472–486
Janićijević Ž, Ninkov M, Kataranovski M, Radovanović F (2019) Poly(dl-lactide-co-ε-caprolactone)/poly(acrylic acid) composite ımplant for controlled delivery of cationic drugs. Macromol Biosci 19(2):1800322
Javed R, Shah LA, Sayed M, Khan MS (2018) Uptake of heavy metal ions from aqueous media by hydrogels and their conversion to nanoparticles for generation of a catalyst system: two-fold application study. RSC Adv 8(27):14787–14797
Jiang G, Qiu W, De Luca PP (2003) Preparation and in vitro/in vivo evaluation of ınsulin-loaded poly(acryloyl-hydroxyethyl starch)-plga composite microspheres. Pharm Res 20(3):452–459
Jv X, Zhao X, Ge H, Sun J, Li H, Wang Q, Lu H (2019) Fabrication of a magnetic poly(aspartic acid)-poly(acrylic acid) hydrogel: application for the adsorptive removal of organic dyes from aqueous solution. J Chem Eng Data 64(3):1228–1236
Karthika JS, Vishalakshi B (2015) Novel stimuli responsive gellan gum-graft-poly(DMAEMA) hydrogelas adsorbent for anionic dye. Int J Biol Macromol 81:648–655
Kaur S, Jindal R (2018) Synthesis of interpenetrating network hydrogel from (gum copal alcohols-collagen)-co-poly(acrylamide) and acrylic acid: isotherms and kinetics study for removal of methylene blue dye from aqueous solution. Mater Chem Phys 220:75–86
Kenawy E-R, Kamoun EA, Mohy Eldin MS, El-Meligy MA (2014) Physically crosslinked poly(vinyl alcohol)-hydroxyethyl starch blend hydrogel membranes: synthesis and characterization for biomedical applications. Arab J Chem 7(3):372–380
Krishnappa PB, Badalamoole V (2019) Karaya gum-graft-poly(2-(dimethylamino)ethyl methacrylate) gel: an efficient adsorbent for removal of ionic dyes from water. Int J Biol Macromol 122:997–1007
Lagergren S (1898) Zur theorie der sogenannten adsorption gelöster stoffe, Kungliga Svenska Vetenskapsakademiens. Handlingar 24(4):1–39
Langmuir I (1918) The adsorption of gases on plane surfaces of glass, mica and platinum. J Am Chem Soc 40(9):1361–1403
Liang L, Li C, Hou T, Zhong Z, Chen D, Li S, Hu Z, Yang H, Ye X (2019) Preparation of poly (allylthiourea-co-acrylic acid) derived carbon materials and their applications in wastewater treatment. Molecules 24(5):957

Mahmoud GA, Abdel-Aal SE, Badway NA, Abo Farha SA, Alshafei EA (2014) Radiation synthesis and characterization of starch-based hydrogels for removal of acid dye. Starch 66(3–4):400–408

Makhado E, Pandey S, Ramontja J (2018) Microwave assisted synthesis of xanthan gum-cl-poly (acrylic acid) based-reduced graphene oxide hydrogel composite for adsorption of methylene blue and methyl violet from aqueous solution. Int J Biol Macromol 119:255–269

Mohamed RR, Elella MHA, Sabaa MW, Saad GR (2018) Synthesis of an efficient adsorbent hydrogel based on biodegradable polymers for removing crystal violet dye from aqueous solution. Cellulose 25:6513–6529

Mohammadian M, Sahraei R, Ghaemy M (2019) Synthesis and fabrication of antibacterial hydrogel beads based on modified-gum tragacanth/poly(vinyl alcohol)/Ag0 highly efficient sorbent for hard water softening. Chemosphere 225:259–269

Mohammed N, Grishkewich N, Berry RM, Tam K (2015) Cellulose nanocrystal–alginate hydrogel beads as novel adsorbents for organic dyes in aqueous solutions. Cellulose 22:3725–3738

Nath J, Chowdhury A, Ali I, Dolui SK (2019) Development of a gelatin-g-poly(acrylic acid-co-acrylamide)–montmorillonite superabsorbent hydrogels for in vitro controlled release of vitamin B12. J Appl Polym Sci 136(22):47596

Ngwabebhoh FA, Gazi M, Oladipo AA (2016) Adsorptive removal of multi-azo dye from aqueousphase using a semi-IPN superabsorbent chitosan-starch hydrogel. Chem Eng Res Design 112:274–288

Ngwabebhoh FA, Mammadli N, Yildiz U (2019) Bioinspired modified nanocellulose adsorbent for enhanced boron recovery from aqueous media: optimization, kinetics, thermodynamics and reusability study. J Environ Chem Eng 7:103281

Ozay H, Ozay O (2013) Rhodamine based reusable and colorimetric naked-eye hydrogel sensors for Fe^{3+} ion. Chem Eng J 232:364–371

Ozay O, Ekici S, Baran Y, Kubilay S, Aktas N, Sahiner N (2010) Utilization of magnetic hydrogels in the separation of toxic metal ions from aqueous environments. Desalination 260(1–3):57–64

Ozay H, Sahin O, Koc OK, Ozay O (2016) The preparation and applications of novel phosphazene crosslinked thermo and pH responsive hydrogels. J Ind Eng Chem 43:28–35

Parlayici S (2019) Alginate-coated perlite beads for the efficient removal of methylene blue, malachite green, and methyl violet from aqueous solutions: kinetic, thermodynamic, and equilibrium studies. J Anal Sci Technol 10:4

Pavithra KG, Kumar PS, Jaikumar V, Rajan PS (2019) Removal of colorants from wastewater: a review on sources and treatment strategies. J Indust Eng Chem 75:1–9

Qi X, Wu L, Su T, Zhang J, Dong W (2018) Polysaccharide-based cationic hydrogels for dye adsorption. Colloids Surf B: Biointerfaces 170:364–372

Sahiner N, Ozay O, Aktas N (2011) 4-Vinylpyridine-based smart nanoparticles with N-isopropylacrylamide, 2-hydroxyethyl methacrylate, acrylic acid, and methacrylic acid for potential biomedical applications. Curr Nanosci 7(3):453–462

Sami AJ, Khalid M, Iqbal S, Afzal M, Shakoori AR (2017) Synthesis and application of chitosan-starch based nanocomposite in wastewater treatment for the removal of anionic commercial dyes. Pak J Zool 49(1):21–26

Sami AJ, Butt YN, Nasar S (2018) Elimination of a carcinogenic anionic dye congo red from water using hydrogels based on chitosan, acrylamide and graphene oxide. J Bioprocess Biotech 8(5):334

Santoso SP, Kurniawan A, Soetaredjo FE, Cheng KC, Putro JN, Ismadji S, Ju YH (2019) Eco-friendly cellulose-bentonite porous composite hydrogels for adsorptive removal of azo dye and soilless culture. Cellulose 26(5):3339–3358

Sharma G, Naushad M, Kumar A, Rana S, Sharma S, Bhatnagar A, Stadler FJ, Ghfar AA, Khan MR (2017) Efficient removal of coomassie brilliant blue R-250 dye using starch/poly(alginic acid-cl-acrylamide) nanohydrogel. Process Saf Environ 109:301–310

Shen W, Jiang X, An QD, Xiao ZY, Zhai SR, Cui L (2019) Combining mussel and seaweed hydrogel-inspired strategies to design novel ion-imprinted sorbents for ultra-efficient lead removal from water. New J Chem 43:5495–5502

Silva A, Sousa E, Palmeira A, Amorim P, Pinho PG, Ferreira DA (2014) Interaction between hydroxyethyl starch and propofol: computational and laboratorial study. J Biomol Struct Dyn 32(11):1864–1875

Singha NR, Karmakar M, Mahapatra M, Mondal H, Dutta A, Roy C, Chattopadhyay PK (2017) Systematic synthesis of pectin-g-(sodium acrylateco-N-isopropylacrylamide) interpenetrating polymer network for superadsorption of dyes/M(II): determination of physicochemical changes in loaded hydrogels. Polym Chem 8:3211–3237

Tang YJ, Yang R, Ma D, Zhou B, Zhu LH, Yang J (2018) Removal of methyl orange from aqueous solution by adsorption onto a hydrogel composite. Polym Polym Compos 26(2):161–168

Thakur S, Arotiba OA (2018) Synthesis, swelling and adsorption studies of a pH-responsive sodium alginate-poly(-acrylic acid) superabsorbent hydrogel. Polym Bull 75(10):4587–4606

Toledo PVO, Limeira DPC, Siqueira NC, Petri DFS (2019) Carboxymethyl cellulose/poly(acrylic acid) interpenetrating polymer network hydrogels as multifunctional adsorbents. Cellulose 26(1):597–615

Wang XL, An WL, Yang Y, Hu ZY, Xu S, Liao W, Wang YZ (2019) Porous gel materials from waste thermosetting unsaturated polyester for high-efficiency wastewater treatment. Chem Eng J 361:21–30

Yang S, Fu S, Li X, Zhou Y, Zhan H (2010) Preparation of salt-sensıtive and antibacterial hydrogel based on quaternized cellulose. BioResources 5(2):1114–1125

Zhu X, Yang R, Gao W, Li M (2017) Sulfur-modified chitosan hydrogel as an adsorbent for removal of Hg(II) from effluents. Fibers Polym 18(7):1229–1234

Zhu C, Xia Y, Zai Y, Dai Y, Liu X, Bian J, Liu Y, Liu J, Li G (2019) Adsorption and desorption behaviors of HPEI and thermoresponsive HPEI based gels on anionic and cationic dyes. Chem Eng J 369:863–873